



N6-Methyladenosine-Related Long Non-coding RNA Signature Associated With Prognosis and Immunotherapeutic Efficacy of Clear-Cell Renal Cell Carcinoma

Tianming Ma^{1,2}, Xiaonan Wang^{2,3}, Jiawen Wang^{1,2}, Xiaodong Liu^{1,2}, Shicong Lai^{1,2}, Wei Zhang¹, Lingfeng Meng^{1,2}, Zijian Tian^{1,2} and Yaoguang Zhang^{1,2*}

¹Department of Urology, Beijing Hospital, National Center of Gerontology, Institute of Geriatric Medicine, Chinese Academy of Medical Sciences, Beijing, China, ²Graduate School of Peking Union Medical College, Chinese Academy of Medical Sciences, Beijing, China, ³Department of Radiology, Beijing Hospital, National Center of Gerontology, Institute of Geriatric Medicine, Chinese Academy of Medical Sciences, Beijing, China

OPEN ACCESS

Edited by:

Jia Meng,
Xi'an Jiaotong-Liverpool University,
China

Reviewed by:

Da Huang,
Shanghai Jiao Tong University School
of Medicine, China

Yao Lin,
Fujian University of Traditional Chinese
Medicine, China

*Correspondence:

Yaoguang Zhang
zhang003887@sina.com

Specialty section:

This article was submitted to
RNA,
a section of the journal
Frontiers in Genetics

Received: 16 June 2021

Accepted: 30 September 2021

Published: 15 October 2021

Citation:

Ma T, Wang X, Wang J, Liu X, Lai S, Zhang W, Meng L, Tian Z and Zhang Y (2021) N6-Methyladenosine-Related Long Non-coding RNA Signature Associated With Prognosis and Immunotherapeutic Efficacy of Clear-Cell Renal Cell Carcinoma. *Front. Genet.* 12:726369. doi: 10.3389/fgene.2021.726369

Increasing evidence suggests that N6-methyladenosine (m6A) and long non-coding RNAs (lncRNAs) play important roles in cancer progression and immunotherapeutic efficacy in clear-cell renal cell carcinoma (ccRCC). In this study, we conducted a comprehensive ccRCC RNA-seq analysis using The Cancer Genome Atlas data to establish an m6A-related lncRNA prognostic signature (m6A-RLPS) for ccRCC. Forty-four prognostic m6A-related lncRNAs (m6A-RLs) were screened using Pearson correlation analysis ($|R| > 0.7$, $p < 0.001$) and univariable Cox regression analysis ($p < 0.01$). Using consensus clustering, the patients were divided into two clusters with different overall survival (OS) rates and immune status according to the differential expression of the lncRNAs. Gene set enrichment analysis corroborated that the clusters were enriched in immune-related activities. Twelve prognostic m6A-RLs were selected and used to construct the m6A-RLPS through least absolute shrinkage and selection operator Cox regression. We validated the differential expression of the 12 lncRNAs between tumor and non-cancerous samples, and the expression levels of four m6A-RLs were further validated using Gene Expression Omnibus data and Lnc2Cancer 3.0 database. The m6A-RLPS was verified to be an independent and robust predictor of ccRCC prognosis using univariable and multivariable Cox regression analyses. A nomogram based on age, tumor grade, clinical stage, and m6A-RLPS was generated and showed high accuracy and reliability at predicting the OS of patients with ccRCC. The prognostic signature was found to be strongly correlated to tumor-infiltrating immune cells and immune checkpoint expression. In conclusion, we established a novel m6A-RLPS with a favorable prognostic value for patients with ccRCC. The 12 m6A-RLs included in the signature may provide new

Abbreviations: AUC, area under curve; ccRCC, clear-cell renal cell carcinoma; C-index, concordance index; DSS, disease-specific survival; GSEA, gene set enrichment analysis; ICI, immune-checkpoint inhibitor; lncRNA, long non-coding RNA; m6A-RL, m6A-related lncRNA; m6A-RLPS, m6A-related lncRNA prognostic signature; OS, overall survival; RNA-seq, RNA-sequencing; ROC, receiver operating-characteristic; TIC, tumor-infiltrating immune cell; TME, tumor microenvironment; TKI, tyrosine kinase inhibitor.

insights into the tumorigenesis and allow the prediction of the treatment response of ccRCC.

Keywords: clear-cell renal cell carcinoma, N6-methyladenosine, lncRNA, prognostic signature, immune infiltration

INTRODUCTION

Kidney cancer, of which renal cell carcinoma (RCC) is the major histological type, is a common type of cancer with a high mortality rate and steadily rising morbidity rate worldwide (Bray et al., 2018). In 2020, there were approximately 73,750 new cases of kidney cancer and approximately 14,830 deaths due to kidney cancer in United States (Siegel et al., 2020). Clear-cell (cc)RCC is the most common subtype of RCC, accounting for more than 70% of cases (Rini et al., 2009). Although surgery is an effective treatment for early-stage ccRCC, relapse or metastasis after curative treatment occurs in 30% of cases. Unfortunately, the prognosis for patients with metastasis is generally dismal because ccRCC is insensitive to conventional radiotherapy and chemotherapy, even to tyrosine kinase inhibitors (TKIs) and immune-checkpoint inhibitors (ICIs) (Ljungberg et al., 2019; Mori et al., 2021). Therefore, it is imperative to elucidate the mechanisms underlying ccRCC development to identify effective treatments.

N6-methyladenosine (m6A), a reversible and abundant modification on mRNAs and non-coding RNAs, has been demonstrated to affect various aspects of RNA metabolism, including splicing, stability, nuclear export, and translation (Huang et al., 2020). Several studies support the hypothesis that aberrant expression of m6A regulators, i.e., “writers” (methyltransferases), “readers” (binding proteins), and “erasers” (demethylases), potentially participates in carcinogenesis, cancer development, or tumor-suppressive activities in various types of cancer, including ccRCC (Wang Q. et al., 2020; Huang et al., 2020). For instance, high expression of methyltransferase 3 (METTL3), an m6A methyltransferase, reportedly promotes the progression of gastric cancer, lung cancer, and prostate cancer (Cai et al., 2019; Wang T. et al., 2020; Wanna-Udom et al., 2020). In contrast, downregulation of METTL3 in endometrial cancer and decreased the expression of alkB homolog 5 (ALKBH5) and fat mass and obesity-associated protein (FTO), which are both “erasers,” in ccRCC, has been suggested to be related to tumorigenicity and dismal prognosis (Liu et al., 2018; Strick et al., 2020).

Long non-coding RNAs (lncRNAs) also actively regulate various biological processes, including tumorigenesis, proliferation, and immunity (Peng et al., 2017; Taniue and Akimitsu, 2021). In ccRCC, lncRNA SNHG1 modulates immune escape by targeting miR-129-3p to activate STAT3 and PD-L1 (Tian et al., 2021), and LINC00641 facilitates ccRCC progression by sponging miR-340-5p (Zhang et al., 2021). Abundant evidence supports that m6A modifications and lncRNAs interactively affect the growth and development of various cancers (Wang X. et al., 2020; Huang et al., 2020; Yang et al., 2020). However, few studies have investigated the exact mechanism by which m6A modifications are involved in

lncRNA-dependent ccRCC progression and prognosis. Recently, several prognostic signatures for ccRCC based on m6A regulators or lncRNAs alone have been identified (Zeng et al., 2019; Chen et al., 2020). However, to the best of our knowledge, an accurate and applicable prognostic signature based on m6A-related lncRNAs for patients with ccRCC has not been formulated. Therefore, we aimed to investigate the prognostic significance of m6A-related lncRNAs (m6A-RLs), and to develop an m6A-related lncRNA prognostic signature (m6A-RLPS) to predict the survival outcomes in patients with ccRCC.

MATERIALS AND METHODS

Data Sources

We collected transcriptome RNA-sequencing (RNA-seq) data of 539 ccRCC samples and 72 adjacent non-tumor samples with corresponding clinical data from the Cancer Genome Atlas (TCGA) database. Detailed clinicopathological information of the patients is provided in **Supplementary Table S1**. Patients with incomplete information were excluded. Expression matrices of 23 m6A-related genes (*METTL3*, *METTL14*, *METTL16*, *WTAPI*, *VIRMA*, *ZC3H13*, *RBM15*, *RBM15B*, *YTHDC1*, *YTHDC2*, *YTHDF1*, *YTHDF2*, *YTHDF3*, *HNRNPC*, *FMR1*, *LRPPRC*, *HNRNPA2B1*, *IGFBP1*, *IGFBP2*, *IGFBP3*, *RBMX*, *FTO*, and *ALKBH5*) were also obtained according to recent publications (Deng et al., 2018; Chen et al., 2019). To validate the expression of target lncRNAs, we extracted gene expression profile data from four datasets with more than 60 ccRCC samples in the Gene Expression Omnibus (GEO) database, including GSE17895 (tumor: $n = 151$, normal: $n = 9$), GSE40435 (tumor: $n = 101$, normal: $n = 101$), GSE46699 (tumor: $n = 67$, normal: $n = 63$), and GSE53757 (tumor: $n = 72$, normal: $n = 72$) (Dalgliesh et al., 2010; Wozniak et al., 2013; Eckel-Passow et al., 2014; von Roemeling et al., 2014). In addition, an updated lnc2Cancer 3.0 (<http://bio-bigdata.hrbmu.edu.cn/lnc2cancer>) database, which hosts comprehensive data on experimentally supported lncRNAs and circular RNAs associated with human cancers (Gao et al., 2021), was used to analyze lncRNA expression further.

m6A-Related lncRNA Identification

The lncRNA profile obtained from TCGA was first screened against the human reference genome (GRCh38. p12; <https://www.ncbi.nlm.nih.gov/genome>). Pearson correlation analysis was used to identify m6A-RLs ($|\text{Pearson's } R| > 0.7$, $p < 0.001$). Then, univariable Cox regression analysis was performed to determine prognostic m6A-RLs related to the overall survival (OS) ($p < 0.01$). The Wilcoxon rank-sum test was utilized to compare the expression levels (visualized using heatmaps) of the prognostic m6A-RLs between tumor and normal tissues.

Consensus Clustering Analysis

To explore the expression features of prognostic m6A-RLs further, we clustered the ccRCC samples into different groups according to the differential expression of the lncRNAs using the ConsensusClusterPlus R package (Chen et al., 2020). Survival analysis and the chi-square test or Fisher's exact test were used to compare the survival rates between the clusters and to determine the relationships between the clinicopathological parameters and the clusters. Heatmaps were created using the "pheatmap" R package to visualize differential expression of the m6A-RLs and clinicopathological parameters in the different groups (Li, 2012).

Gene Set Enrichment Analysis and Tumor-Infiltrating Immune Cell Profiling

GSEA was conducted using the Hallmark, C2 KEGG v.7.1, C5 GO, and C7 v.6.2 gene sets in GSEA v.4.0.3 (<http://www.broadinstitute.org/gsea>) to investigate potential m6A-RL pathways and functions. The ESTIMATE algorithm was used to determine immune, stromal, and ESTIMATE scores for each sample. These scores represent the ratios of immune and stromal components and the total proportion of these components in the tumor microenvironment (TME) (Yoshihara et al., 2013). The CIBERSORT algorithm was used to estimate the abundance of 22 tumor-infiltrating immune cells (TICs) (Chen et al., 2018). Only tumor samples with $p < 0.05$ were retained for subsequent analysis.

Analysis of the Associations Between Clusters and Tumor-Infiltrating Immune Cells

The Wilcoxon rank-sum test was used to determine the relationships between TICs in the different clusters. Some common immune checkpoints, including CTLA-4, LAG-3, HAVCR2 (TIM-3), PDCD1 (PD-1), and TIGIT, were screened out to compare differences in expression between tumor and normal tissues and in the differential clusters, as well as to investigate the correlations between the expression levels of the genes and hub m6A-RLs.

Establishment and Validation of the m6A-Related LncRNA Prognostic Signature

The entire cohort was randomly divided into training and first validation groups at a 1:1 ratio. Thereafter, all the samples were randomly divided into the second and third validation cohorts at a ratio of 3:7. The training cohort was used to construct the m6A-RLPS to predict the prognosis of ccRCC patients. The selected m6A-related candidate lncRNAs mentioned above were subjected to least absolute shrinkage and selection operator (LASSO) Cox regression analysis for establishing an m6A-RLPS for ccRCC (Friedman et al., 2010). A risk score was then calculated for each patient using the following formula: $\text{risk score} = \sum_{i=1}^n \text{Coef}_i * \text{Expr}_i$, where Coef_i is the coefficient and Expr_i is the expression value of the i th lncRNA in the signature. Univariable Cox regression

and Kaplan–Meier survival analyses were used to analyze the prognostic significance of the selected lncRNAs and their co-expressed m6A genes. The Wilcoxon rank-sum test was used to investigate differential expression of the selected lncRNAs and co-expressed m6A genes between tumor and non-cancerous samples in TCGA, which was further validated using GEO datasets and Lnc2Cancer 3.0.

Next, patients were classified into low- and high-risk groups according to the median risk score. The OS and disease-specific survival (DSS) were compared between the groups based on Kaplan–Meier curves. Time-dependent receiver operating-characteristic (ROC) curves with area under curve (AUC) values for the 1-, 3-, and 5-years OS and DSS rates were used to estimate the prognostic prediction efficacy of the m6A-RLPS. Heatmaps were generated to visualize the differential expression of the prognostic m6A-RLs in the low- and high-risk groups. Univariable and multivariable Cox regression analyses were used to investigate the independent predictive value of the risk score and clinicopathological parameters for the survival of patients with ccRCC. Survival analysis was conducted to further elucidate the prognostic ability of the risk score in subgroups stratified by age, sex, grade, clinical stage, and T stage. A nomogram was built based on the multivariate Cox regression analysis results and was comprehensively evaluated using the concordance index (C-index) and calibration curves.

Correlation Between the m6A-Related LncRNA Prognostic Signature and Clinicopathological Parameters

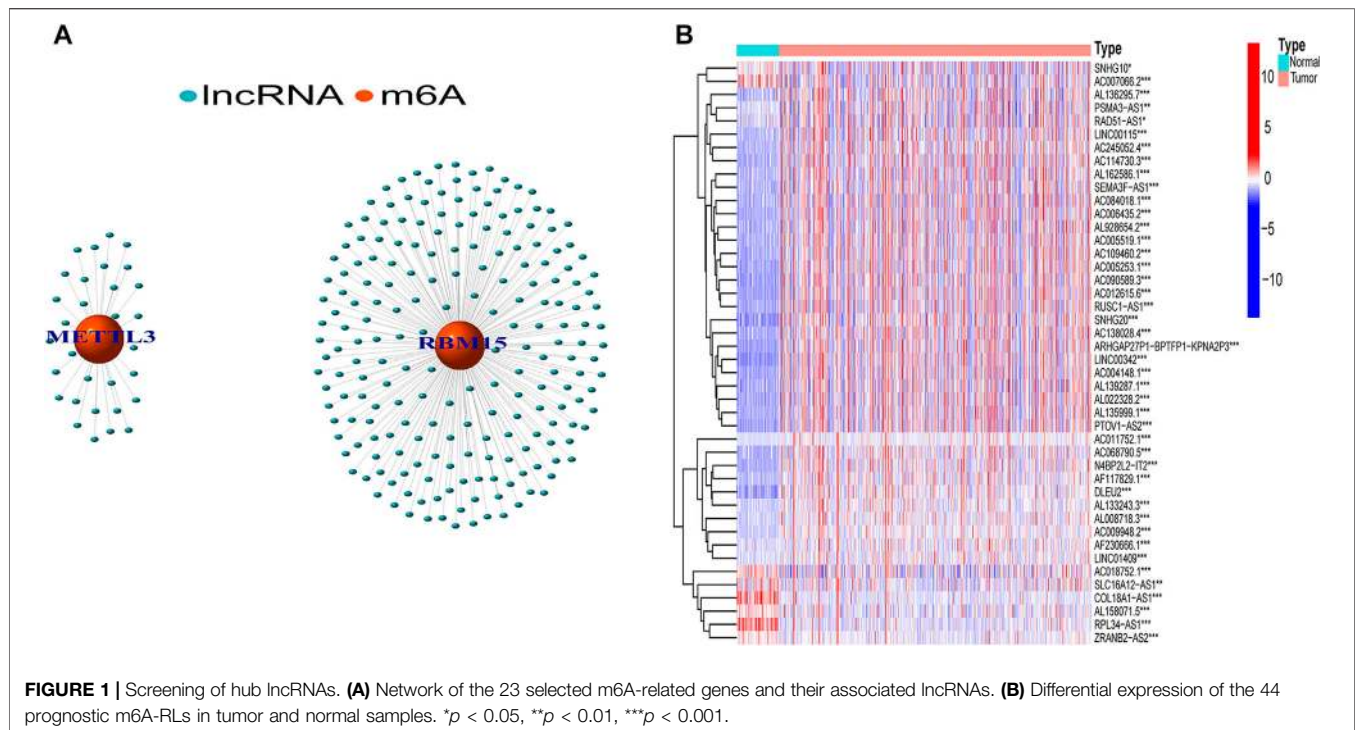
Associations between the clinicopathological parameters, immune score, clusters, and m6A-RLPS risk levels were assessed using the chi-square test or Fisher's exact test (shown in heatmaps). Student's t -test was used to determine the relationships between the risk scores and clinicopathological parameters, including age, sex, grade, clinical stage, T stage, cluster, immune score, stromal score, and ESTIMATE score. Additionally, survival analysis was employed to explore associations between all these factors and patient OS.

Correlation Between the m6A-Related LncRNA Prognostic Signature and Immune-Related Features

Correlations between the m6A-RLPS and immune cells were evaluated using the Wilcoxon rank-sum test and Spearman correlation analysis. In addition, we downloaded data of different cancer cell lines from the NCI-60 database (<https://discover.nci.nih.gov/cellminer/home.do>). Thereafter, the m6A-RLPS was also comprehensively analyzed to determine its relationship with the expression of some immune checkpoint proteins and drug sensitivity of some TKIs involved in ccRCC.

Statistical Analysis

All analyses were performed using R v.4.0.3 (<http://www.R-project.org>). The Wilcoxon rank-sum test was used to



investigate differential expression of lncRNAs and TICs. The Pearson correlation analysis was performed to identify m6A-RLs. Kaplan-Meier method and log rank test were used for comparing the OS and DSS between various groups, incorporating the high and low-risk groups and other subgroups based on the expression of each of the 12 m6A-RLs. Student's *t*-test was used to determine the relationships between the risk scores and clinicopathological parameter. Chi-square test or Fisher's exact test was used to analyze associations between the clinicopathological parameters, immune score, clusters, and m6A-RLPS. Univariable and multivariable Cox regression analyses were applied to investigate the independent predictive value of the m6A-RLPS for the OS and DSS of patients with ccRCC. Statistical significance was set at $p < 0.05$ (two-tailed).

RESULTS

Identification of Prognostic m6A-RLs in Clear-Cell Renal Cell Carcinoma

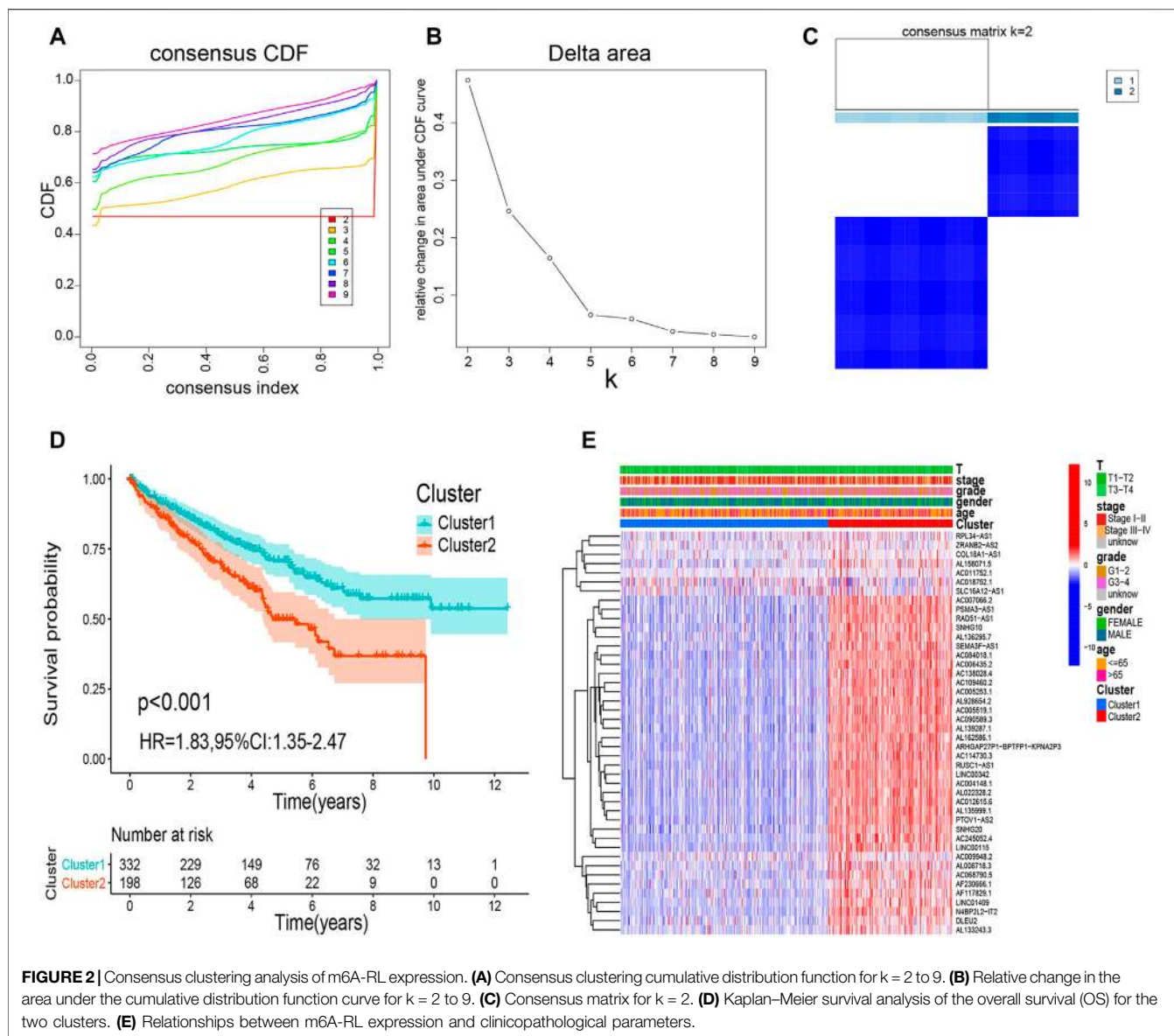
In total, 239 m6A-related lncRNAs were found to be significantly correlated with 23 m6A-related genes using Pearson correlation analysis ($|R| > 0.7$, $p < 0.001$, **Figure 1A**, **Supplementary Table S2**). After excluding patients without cancer or survival data, we merged the survival data with lncRNA expression data of each patient (final patient number = 530). Then, we identified 44 lncRNAs related to prognosis ($p < 0.01$, **Supplementary Table S3**) using univariable Cox regression analysis. As shown in **Figure 1B**, the expression of these prognostic m6A-RLs differed significantly between normal and ccRCC tissues.

Consensus Clustering of m6A-Related lncRNAs Identified in Molecular Subtypes Clear-Cell Renal Cell Carcinoma

We categorized all samples into groups according to the expression profiles of the prognostic m6A-RLs, using a consensus clustering algorithm. We found that $k = 2$ was the most suitable choice to sort the entire cohort into two groups: cluster 1 ($n = 332$) and cluster 2 ($n = 198$) (**Figures 2A–C**). Kaplan-Meier curves revealed that patients in cluster 2 had a worse OS than those in cluster 1 ($p < 0.001$, **Figure 2D**). Nevertheless, as shown in **Figure 2E**, there were no distinct differences in clinical variables (age, sex, grade, clinical stage, and T stage) between the clusters. Thus, the consensus clustering results were clearly associated with the survival of patients with ccRCC.

GSEA and Immune-Related Analysis of the Two Clusters

To determine the potential pathways and functions associated with the prognostic m6A-RLs in ccRCC, GSEA was applied to the two clusters. Notably, several tumor hallmarks, such as coagulation, glycolysis, and mTORC1 signaling, were predominantly enriched in cluster 1 (nominal $p < 0.05$ and false discovery rate-corrected $q < 0.05$, **Figure 3A**). C2 Kyoto Encyclopedia of Genes and Genomes (KEGG) and C5 Gene Ontology (GO) analyses similarly revealed multiple tumor-related signaling pathways in the samples (**Figures 3B,C**). Notably, several enriched immune-related signaling pathways and genes were identified through both C2 KEGG and C5 GO



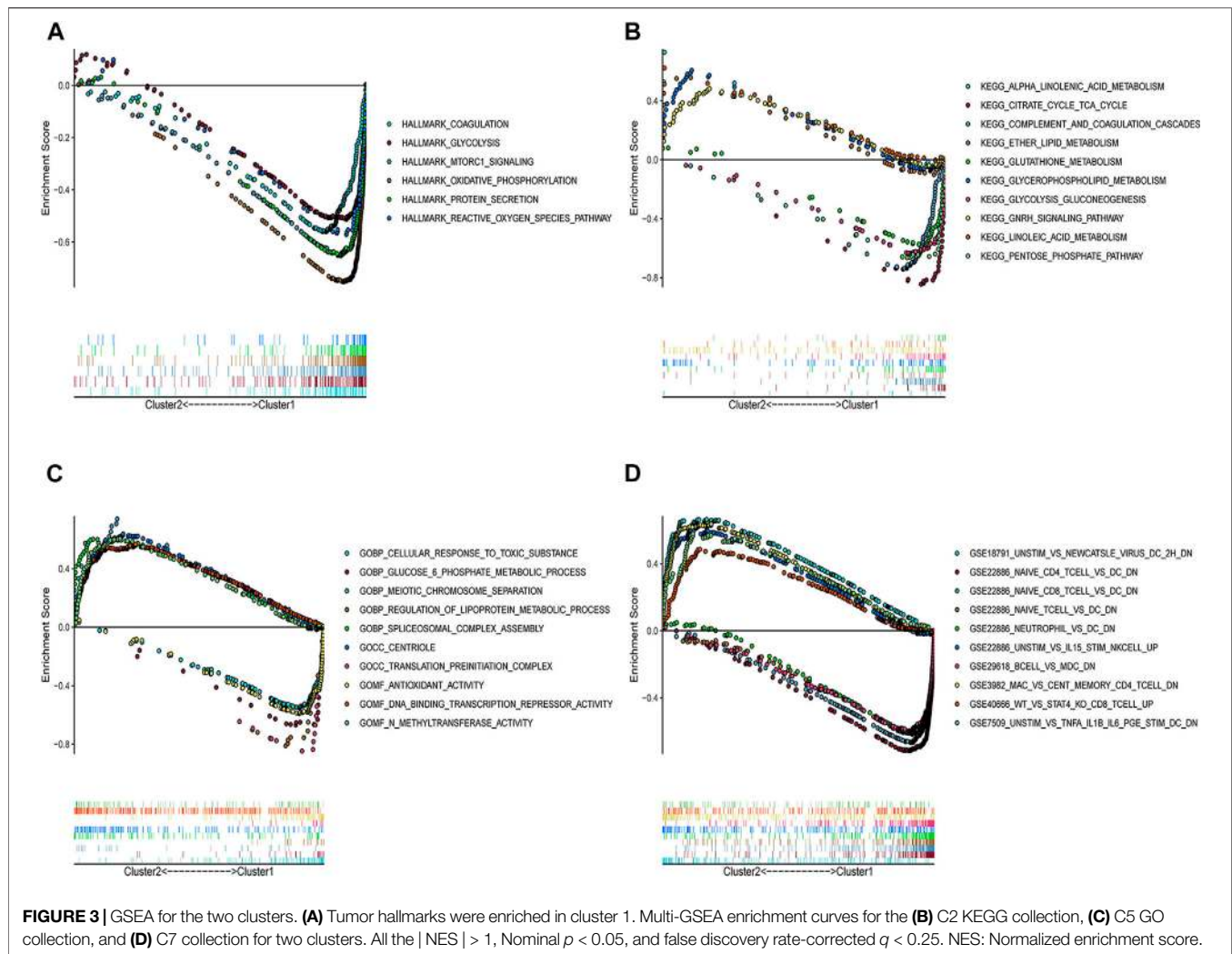
analyses. C7 collection analysis indicated that multiple immune-functional gene sets were enriched in clusters 1 and 2 (Figure 3D).

Additionally, we thoroughly evaluated the correlations between the two clusters and TICs in the ccRCC samples. Activated dendritic cells, activated memory CD4 T cells, CD8 T cells, follicular helper T cells, gamma delta T cells, M0 macrophages, naive B cells, neutrophils, and resting natural killer cells were significantly associated with the clusters (Figure 4A). Given the potential immunomodulatory effects of the expression of the m6A-RLs, we determined the correlations between the clusters and some immune checkpoints. Notably, all five immune checkpoints evaluated, except TIM-3, were highly expressed in tumor samples and cluster 2 (Figure 4B). The correlations between the 44 lncRNAs and the five immune checkpoints are shown in Supplementary Figure S1, and

most of these correlations were significant. Based on these results, we speculated that the poor prognosis of patients in cluster 2 was probably due to the upregulation of the immune checkpoints.

Construction and Validation of the m6A-Related LncRNA Prognostic Signature

The entire cohort with complete survival information was randomly divided into training ($n = 266$) and the first validation ($n = 264$) cohort at a ratio of 1:1 and was then divided into the second ($n = 156$) and third ($n = 374$) validation cohorts at a ratio of 3:7. The risk model was developed using the training cohort and validated using the validation cohorts. We conducted LASSO Cox regression analysis to screen the 44 prognostic m6A-RLs and the 12



lncRNAs incorporated into the m6A-RLPS for lncRNAs that would allow prediction of the OS of patients with ccRCC (Figures 5A–C). The risk score for each patient was calculated as follows: risk score = $(1.083 \times AC009948.2 \text{ expression}) + (-0.303 \times AC011752.1 \text{ expression}) + (-0.148 \times AC018752.1 \text{ expression}) + (-0.002 \times AF117829.1 \text{ expression}) + (0.616 \times AL008718.3 \text{ expression}) + (0.334 \times AL133243.3 \text{ expression}) + (-0.943 \times AL158071.5 \text{ expression}) + (-0.363 \times COL18A1-AS1 \text{ expression}) + (0.141 \times DLEU2 \text{ expression}) + (0.217 \times LINC00115 \text{ expression}) + (-2.645 \times RPL34-AS1 \text{ expression}) + (0.053 \times SNHG10 \text{ expression})$ (expression refers to the normalized log levels of each lncRNA). Both univariable Cox regression analysis and Kaplan–Meier log-rank test-based survival analysis supported the remarkable prognostic significance of all 12 lncRNAs, among which AC011752.1, AC018752.1, AL158071.5, COL18A1-AS1, and RPL34-AS1 were protective factors with a hazard ratio < 1 , whereas all others were risk factors (Figure 5D–P).

The relative expression levels of the 12 signature lncRNAs differed significantly between normal and ccRCC tissues based on TCGA data (Figures 6A,B). In addition, we collected the

expression data from the GEO DataSets platform for validation analysis of the 12 lncRNAs. Ultimately, only GSE17895 (contained DLEU2), GSE40435 (contained DLEU2, LINC00115, and SNHG10), GSE46699 and GSE53757 (both contained COL18A1-AS1, DLEU2, LINC00115, and SNHG10) were included in the subsequent analyses. The results showed that DLEU2 and LINC00115 were markedly overexpressed in ccRCC samples compared with normal tissues, whereas the expression levels of COL18A1-AS1 and SNHG10 were remarkably lower in tumor tissues than those in the adjacent non-tumor samples (Figure 6C–N). Furthermore, Wilcoxon rank-sum test in Lnc2Cancer 3.0 showed the similar differential expression of COL18A1-AS1, DLEU2, LINC00115, RPL34-AS1, and SNHG10 (Supplementary Figure S2). These findings were in accordance with the results of TCGA analysis. Moreover, the co-expression of m6A genes (*METTL3* and RNA binding motif protein 15 (*RBM15*)) of the 12 lncRNAs also differed between tumor and normal tissues and was associated with OS in ccRCC (Supplementary Figure S3).

Next, the patients were classified into high- and low-risk groups based on the median m6A-RLPS risk score.

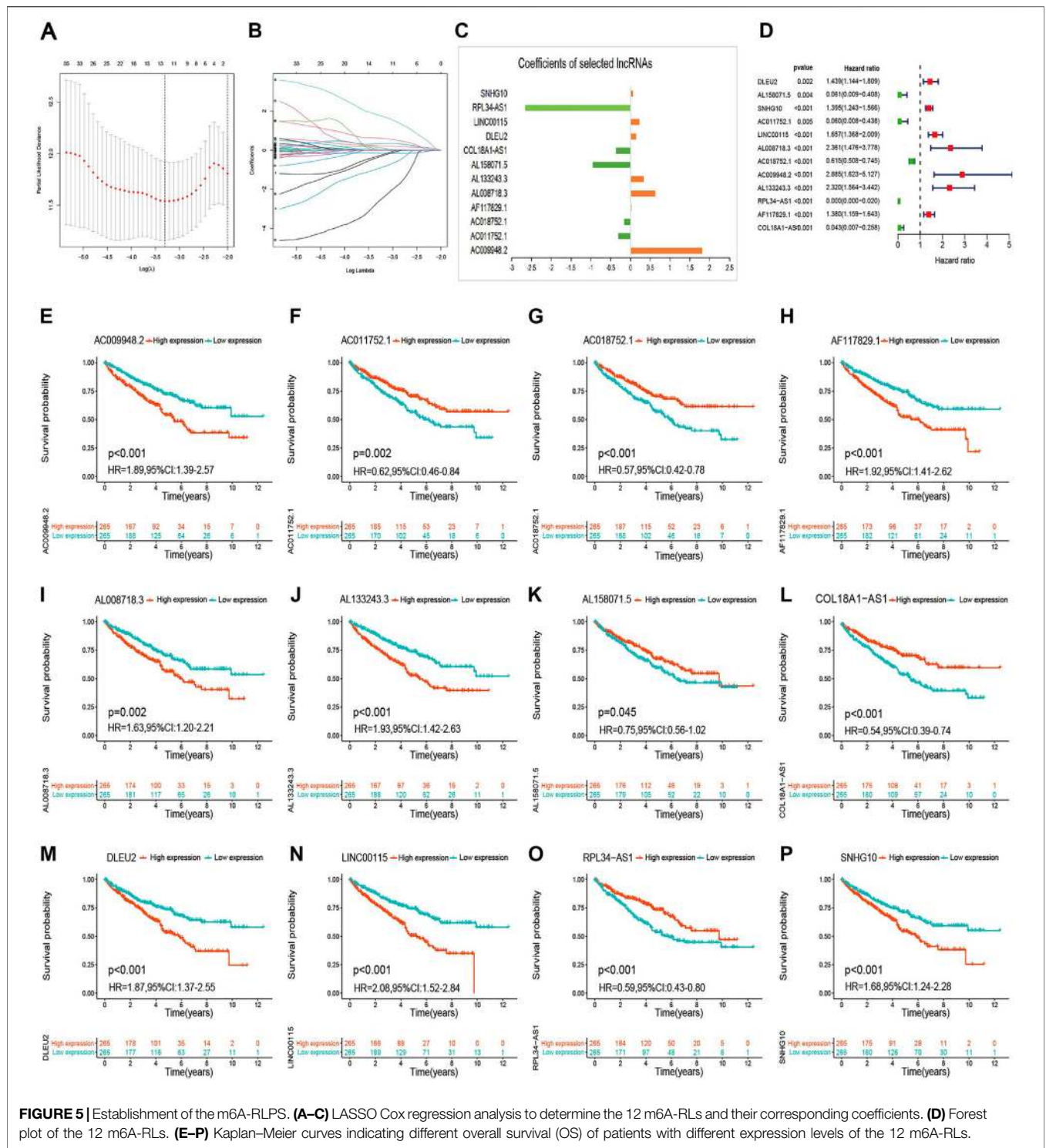
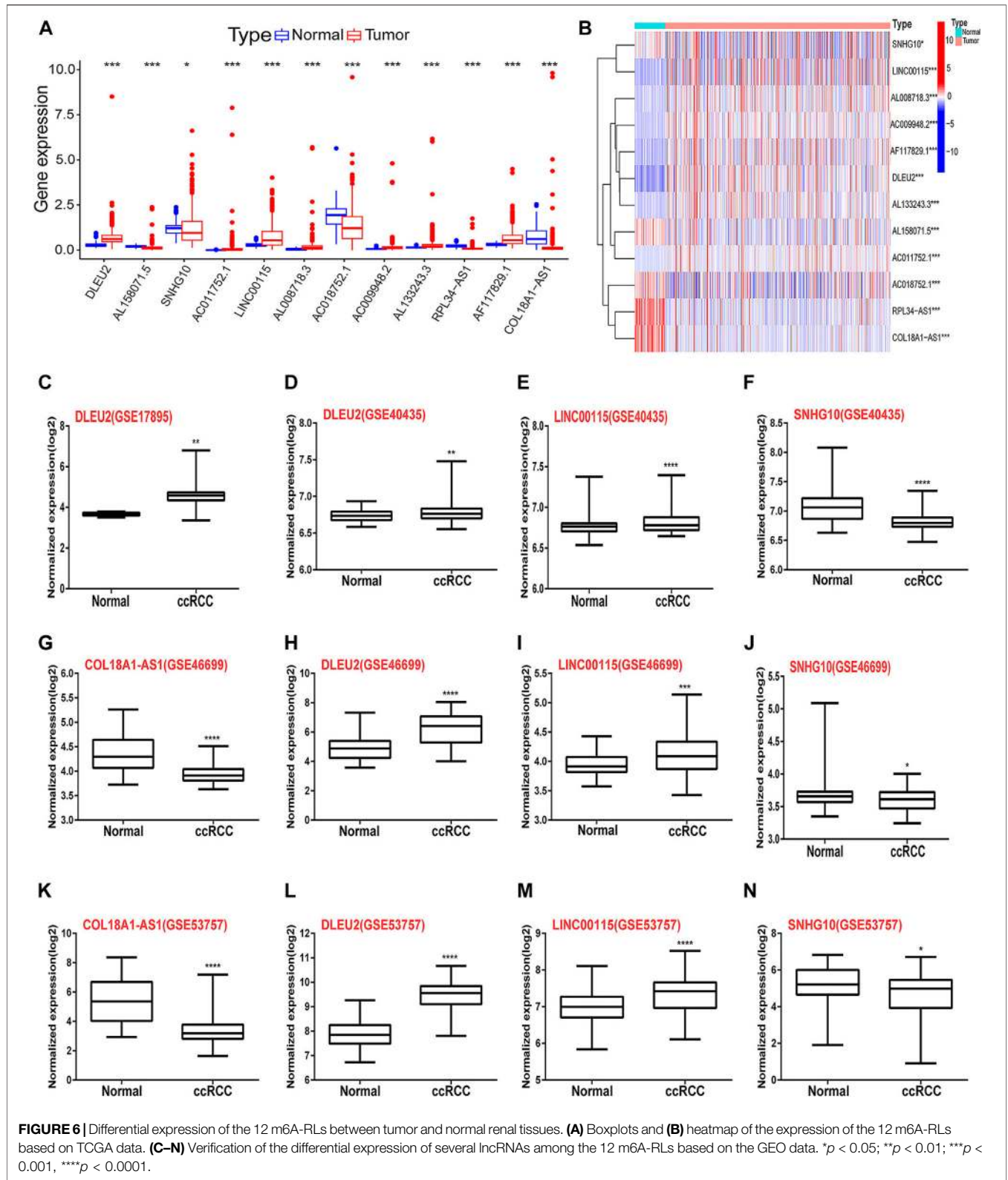


FIGURE 5 | Establishment of the m6A-RLPS. **(A–C)** LASSO Cox regression analysis to determine the 12 m6A-RLs and their corresponding coefficients. **(D)** Forest plot of the 12 m6A-RLs. **(E–P)** Kaplan–Meier curves indicating different overall survival (OS) of patients with different expression levels of the 12 m6A-RLs.

multivariate analysis validated that these four variables were independent prognostic factors in patients with ccRCC (Figures 8A–D, Supplementary Figure S6A–D). Tests for interaction revealed no significant association between the effect of risk score and clinicopathological factors on the OS and DSS (all *p* values for interactions > 0.05) (Supplementary

Table S4). Stratification survival analysis to estimate the predictive ability of m6A-RLPS in ccRCC patients with different clinicopathology revealed that high-risk patients had a worse OS and DSS than low-risk patients in every subgroup (Figure 8E–N, Supplementary Figure S6E–N), indicating the good predictive performance of the m6A-RLPS.



A nomogram for the 3- and 5-years OS rates based on the independent predictors determined using the multivariate analysis are shown in **Supplementary Figure S7A**. A point

was plotted for each covariate, and a total nomogram score correlated with the 3- and 5-years OS rates was calculated for each patient. The nomogram showed a favorable accuracy in

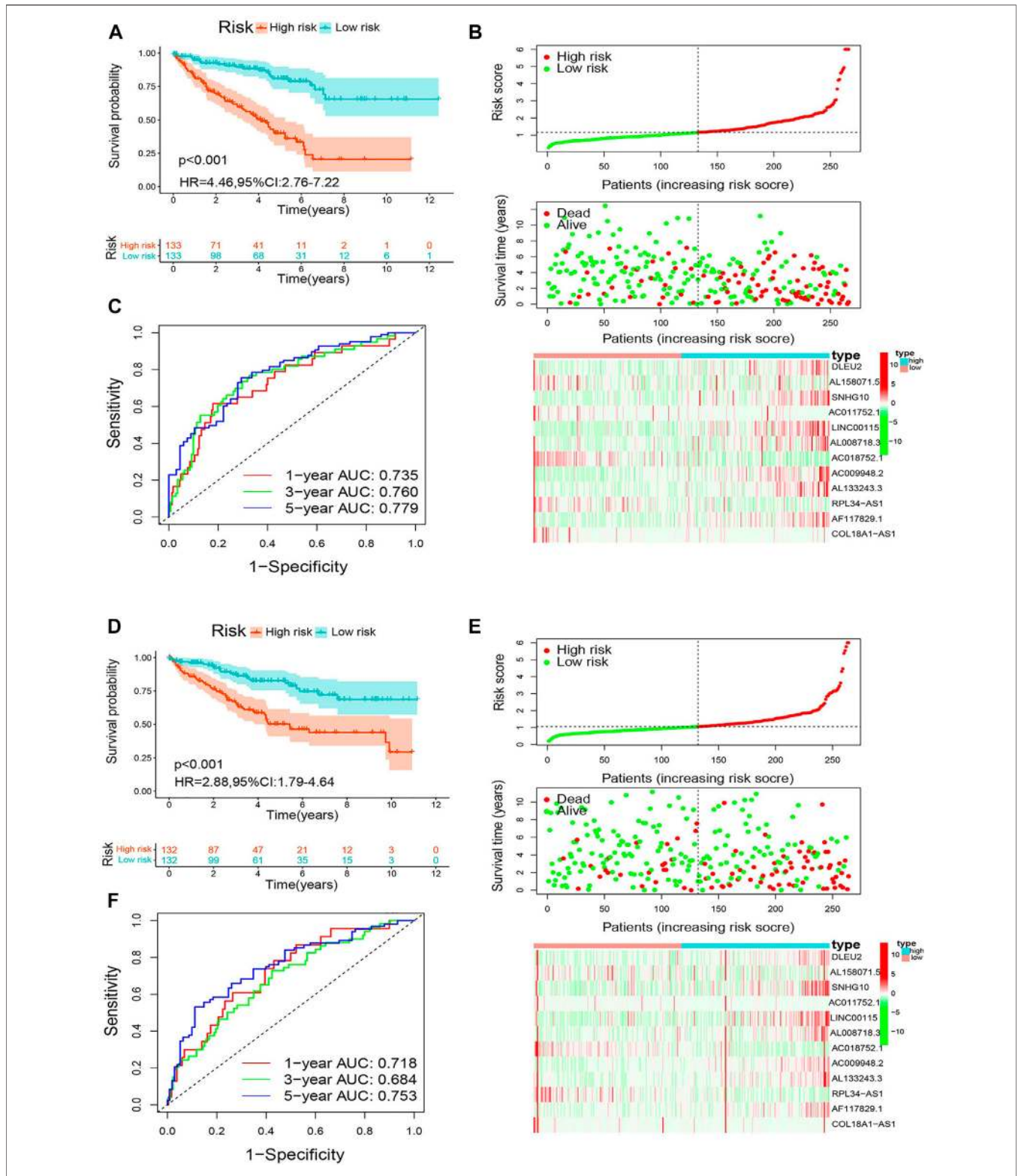
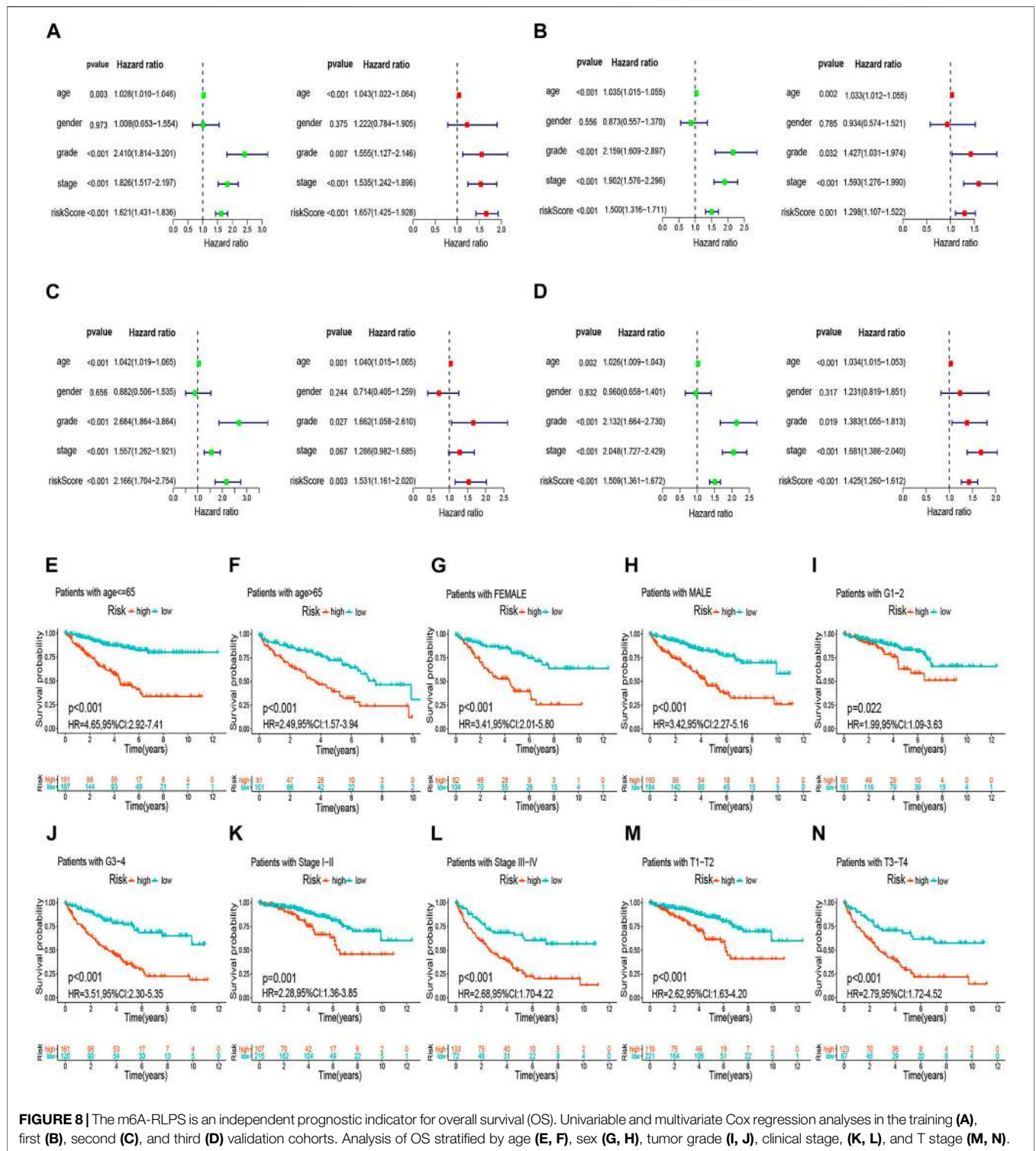
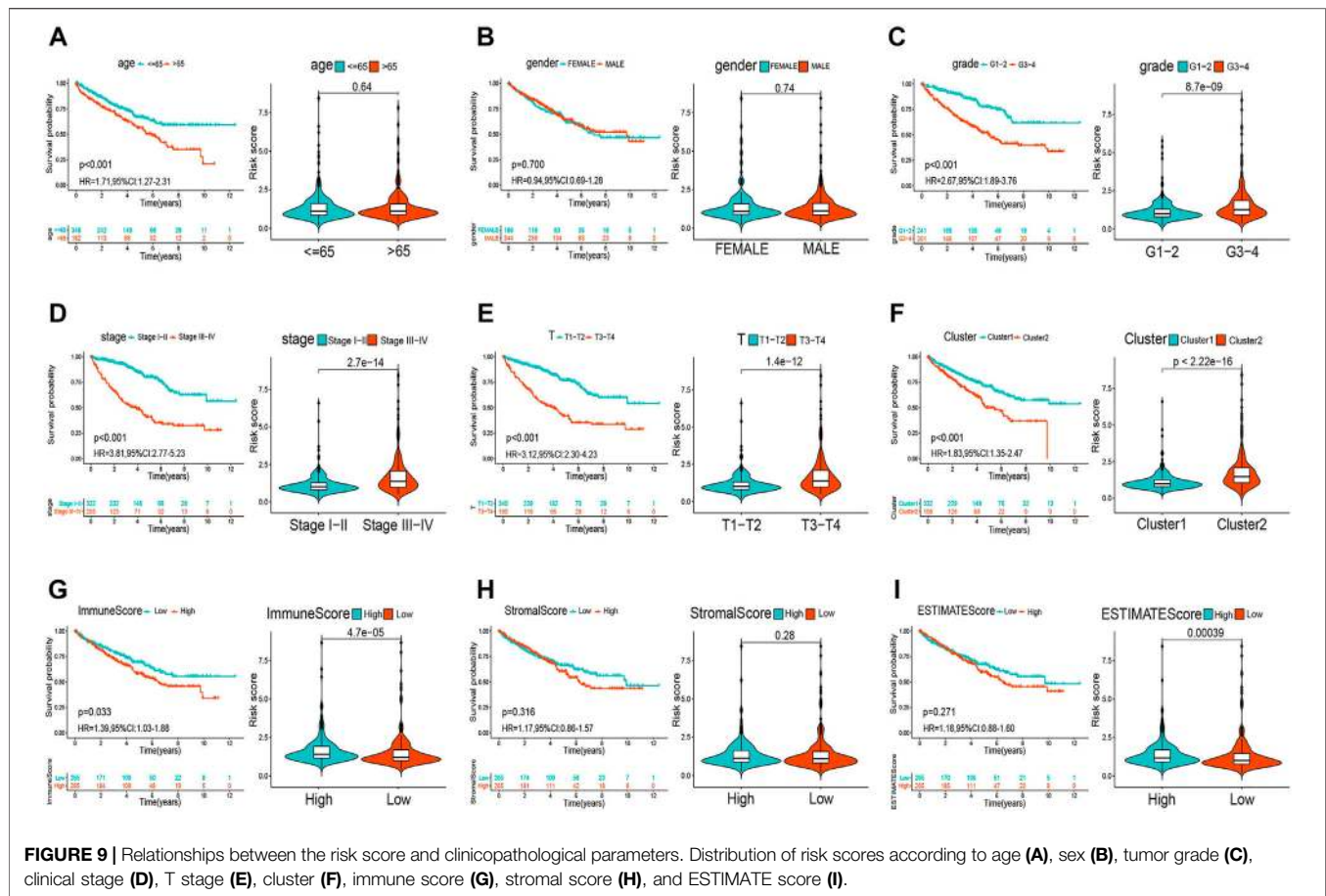


FIGURE 7 | Analysis of the m6A-RLPS efficacy in patients stratified by risk level. **(A)** Kaplan–Meier curves of overall survival (OS) for the m6A-RLPS **(B)** Distributions of risk scores, survival status, and relative lncRNA expression; and **(C)** ROC curves for predicting 1-, 3-, and 5-years OS rates in the training cohort. **(D)** Kaplan–Meier curves of OS for the m6A-RLPS **(E)** Distributions of risk scores, survival status, and relative lncRNA expression; and **(F)** ROC curves for predicting 1-, 3-, and 5-years OS rates in the first validation cohort.



predicting OS, with a C-index of 0.80 (95% CI: 0.76–0.84), 0.76 (95% CI: 0.70–0.82), 0.78 (95% CI: 0.72–0.84), and 0.78 (95% CI: 0.74–0.82) for the training, first, second, and third validation cohorts, respectively. Moreover, calibration curves revealed that

there was an appreciable agreement between the predictive outcome and actual survival, and similar findings were obtained in the validation cohorts (Supplementary Figure S7B–I).



The m6A-Related lncRNA Prognostic Signature Correlates With Clinicopathology and TME Immune Activity

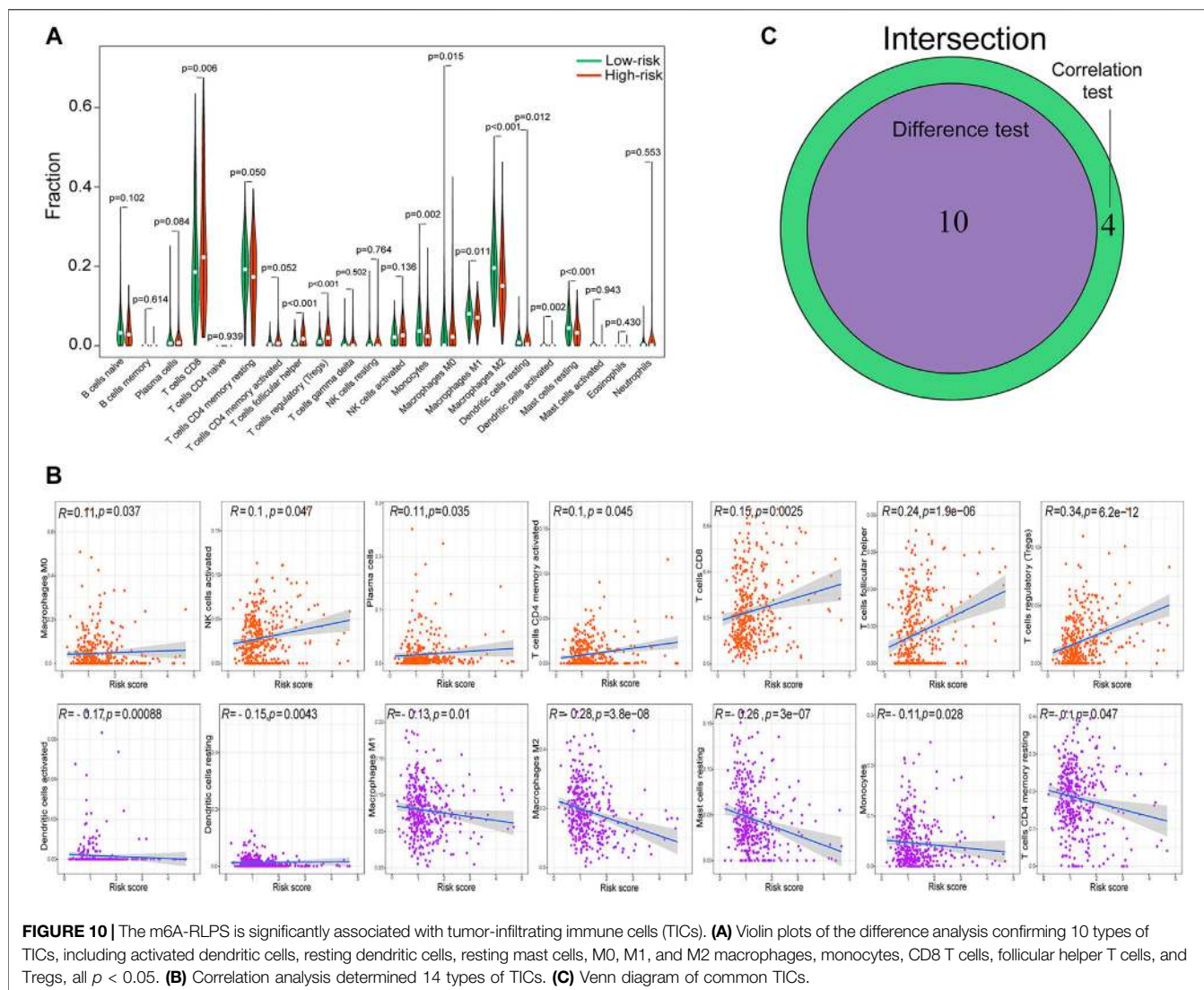
The heatmap in **Supplementary Figure S8** shows that the expression of the lncRNAs included in the m6A-RLPS was significantly correlated with cluster type, immune score, tumor grade, tumor stage, and T stage (all $p < 0.01$). In addition, a Student t -test revealed that the risk score increased with increasing tumor grade, clinical stage, T stage, immune score, and ESTIMATE score (**Figures 9A–E, G–I**), and that high-risk patients tended to be classified into cluster 2 (**Figure 9F**). These findings suggested that the lncRNAs included in the m6A-RLPS can influence the progression, malignancy, and survival outcomes of ccRCC.

Given the strong association between clinicopathology and TME immune activity, we comprehensively investigated the correlation between the m6A-RLPS risk score and immune cell infiltration. By combining difference and correlation analyses, we found that 10 types of TICs, including activated dendritic cells, resting dendritic cells, resting mast cells, M0, M1, and M2 macrophages, monocytes, CD8 T cells, follicular helper T cells, and regulatory T cells (Tregs), were strikingly associated with the m6A-RLPS (**Figure 10**). Of these cell types, four were positively correlated with the m6A-RLPS (M0 macrophages, CD8 T cells, follicular helper T cells, and Tregs), whereas the others were negative correlated.

Finally, we compared drug sensitivity to some TKIs, including axitinib, pazopanib, sorafenib, and sunitinib, between the risk groups. The risk stratification was significantly associated with pazopanib and sunitinib sensitivity (**Figure 11A**). In addition, the m6A-RLPS had a strong positive correlation with the TME scores obtained using the ESTIMATE algorithm (**Figure 11B**). Given the significant correlations of the routine immune checkpoints with the clusters, we next explored the associations between the m6A-RLPS and these immune checkpoints. The expression levels of all immune checkpoints, except TIM-3, were increased in high-risk patients and positively correlated with the risk score, reflecting the effect of the immune checkpoints on the TME and poor oncological outcomes (**Figures 11C,D**).

DISCUSSION

Due to the complexity and heterogeneity of ccRCC, patients with ccRCC generally have a high risk of recurrence and metastasis, as well as a dismal prognosis (Shingarev and Jaimes, 2017). Because of the limited predictive capability of traditional prognostic models, an m6A-related lncRNA-based prognostic model may improve the understanding and management of ccRCC (Veeratterapillay et al., 2012). Therefore, in this study, by systematically screening and identifying target lncRNAs, we

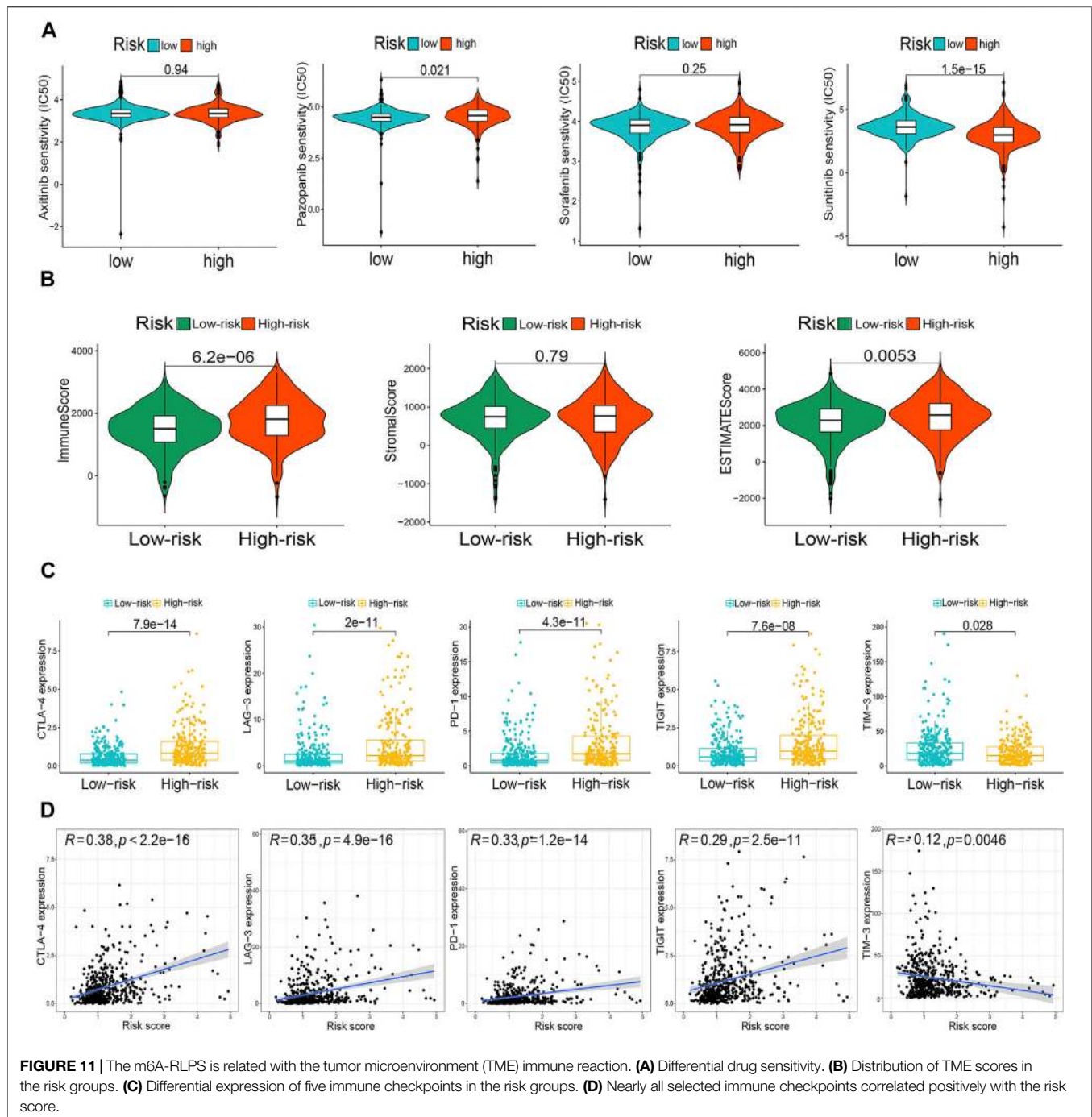


created a reliable prognostic model with a satisfactory predictive capability for ccRCC outcomes.

We conducted a comprehensive ccRCC RNA-seq analysis using data of 539 patients with ccRCC downloaded from TCGA database. In total, 239 m6A-RLs were filtered out, 44 of which were determined to have prognostic value. Next, we divided all ccRCC samples into two clusters by consensus clustering to shed light on the potential effects of the m6A-RLs. The cluster subtypes were strongly linked to the OS of the patients with ccRCC, and cluster 2, comprising patients with worse prognosis, was associated with malignancy-related signaling pathways and numerous immune-related activities as indicated by GSEA. Further analyses emphasized the close relationships among the m6A-RLs, TICs, and immune checkpoints, which indicated that the expression pattern of m6A-RLs is remarkably associated with immunity and oncogenesis. Twelve lncRNAs of the forty-four m6A-RLs were used to construct an m6A-RLPS, which stratified the patients with ccRCC into low- and high-risk groups and exhibited a substantial prognostic prediction performance. The expression of four lncRNAs (COL18A1-AS1, DLEU2, LINC00115, and SNHG10) of the 12 m6A-RLs in ccRCC

and normal tissues was evaluated using the GEO data. Multivariate Cox regression analysis showed that the m6A-RLPS was an independent prognostic factor for OS and DSS, and the prognostic predictive capacity of the signature was validated in patients stratified according to clinicopathological parameters. By integrating the m6A-RLPS, age, and tumor grade and stage, we constructed a quantitative nomogram, which was highly accurate and reliable in estimating patient survival. In fact, previous studies have also shown some novel prognostic signatures of ccRCC. Zeng et al. (2019) constructed a prognostic model based on six-lncRNAs, and Chen et al. (2020) identified an m6A RNA methylation regulator-based signature, which were used for predicting the OS of ccRCC and showed a good prediction efficiency, consistent with our model. However, each of the previous studies mainly focused on differentially expressed lncRNAs or m6A regulators; they did not combine and explore the association between m6A modification and lncRNAs, and did not validate the efficacy of signature in predicting DSS of ccRCC.

Numerous studies have highlighted the fact that m6A modification in specific lncRNAs affects tumorigenesis and



metastasis in cancer through various mechanisms; however, how it affects particular lncRNAs in ccRCC remains unclear. In hepatocellular carcinoma, METTL3-mediated m6A modification stabilizes the lncRNA LINC00958 transcript to increase the levels of hepatoma-derived growth factor, thus facilitating tumor growth (Zuo et al., 2020). YTHDF3 inhibits colorectal cancer progression by negatively modulating the lncRNA GAS5 to generate a GAS5-YAP-YTHDF3 negative feedback loop (Ni et al., 2019). Furthermore, lncRNAs can interact with m6A regulators to regulate their functions. For example, the lncRNA GAS5-AS1 enhances the

stability of GAS5 by interacting with ALKBH5 to suppress the proliferation of cervical cancer (Wang et al., 2019). We found METTL3 to be a risk factor associated with poor prognosis of ccRCC, which was consistent with findings in one previous study, but in contrast to those in another study (Li et al., 2017; Chen et al., 2020); thus, the role of METTL3 in ccRCC remains uncertain. Moreover, studies have revealed that METTL3 and RBM15/15B can modulate m6A modification of lncRNA-XIST, which has been shown to facilitate ccRCC tumorigenicity via the miR-302c/SDC1 axis (Patil et al., 2016; Zhang et al., 2017). Together, the findings

suggest that interactions between m6A modification and lncRNAs play vital roles in cancer development and improve our understanding of ccRCC and may aid in identifying potential prognostic markers for this disease.

Among the 12 prognostic m6A modification-related lncRNAs included in the m6A-RLPS, DLEU2 has been associated with the prognosis of multiple types of cancers (Ghafouri-Fard et al., 2021). Chen et al. (2017) reported that DLEU2 downregulates miR-30a-5p, resulting in poor prognosis in patients with ccRCC. LINC00115 can target miR-489-3p through the PI3K/AKT/mTOR pathway to promote the progression of colorectal cancer (Feng et al., 2020), and it can be activated by TGF- β to regulate the tumorigenicity of glioblastoma (Tang et al., 2019). Zhu et al. (2020) reported that lncRNA SNHG10 contributes to the proliferation and invasion of osteosarcoma by activating Wnt/ β -catenin signaling via sponging miR-182-5p. Yuan et al. (2020) suggested that SNHG10 accelerates gastric cancer cell proliferation and migration via targeting the miR-495-3p/CTNBN1 axis. Unfortunately, to date, only few studies have been conducted in ccRCC, and the remaining nine lncRNAs have been rarely studied. However, our results corroborate the prognostic value of these m6A-targeted lncRNAs and offer insights into their potential roles in ccRCC oncogenesis and progression.

There is increasing evidence for the significance of m6A modification and lncRNAs in the regulation of cancer immunity, including immune cell infiltration in the TME, and immune resistance and activation (Denaro et al., 2019; Gu et al., 2021). The TME plays an important role in the tumorigenesis and progression of ccRCC (Hinshaw and Shevde, 2019). Recently, ICIs combined with TKIs have been recommended as a first-line treatment for metastatic RCC and the TME is actively involved in the therapeutic efficacy of these treatments (Simonaggio et al., 2021). Our findings indicated that the m6A-RLs play vital roles in ccRCC immune status. Therefore, we thoroughly analyzed the association between the m6A-RLPS and TME immune activity. The results showed that the risk score was strongly related with the TME score. Among TICs, the levels of M0 macrophages, CD8 T cells, follicular helper T cells, and Tregs notably differed between the high- and low-risk groups and were positively correlated with the risk score. Notable, these TICs reportedly are associated with tumorigenesis, progression, and immunotherapy efficacy in ccRCC (Santagata et al., 2017; Kadamoto et al., 2019; Xiong et al., 2020). Recent studies focusing on immune checkpoints, such as CTLA-4, LAG-3, PD-1, TIGIT, and TIM-3, have uncovered that these can significantly regulate the cancer immune function of TICs, leading to the inhibition of immune surveillance (Carosella et al., 2015; Manieri et al., 2017; Andrews et al., 2019). Therefore, immunotherapy has emerged as a promising cancer therapeutic option, and the clinical utility of combinations of ICIs and TKIs in metastatic ccRCC is being extensively researched (Motzer et al., 2019; Powles et al., 2020). In our study, the risk subgroups were notably related to the sensitivity to pazopanib and sunitinib. More importantly, the expression levels of nearly all the above immune checkpoints were positively correlated with the risk score calculated with the prognostic signature, suggesting that an immunosuppressive microenvironment is causally related with poor prognosis, and indicating the potential utility of our m6A-RLPS in estimating the response to ICIs.

We employed and analyzed clinical and survival data from a large cohort of patients with ccRCC from the TCGA database and validated

the differential expression of several lncRNAs between normal and tumor tissues based on the GEO data. Nonetheless, this study had some limitations. First, because of a lack of ccRCC samples and large independent clinical data, we were not able to clinically validate the findings. In addition, the detailed functional roles of the m6A-related lncRNAs in ccRCC remain to be identified.

In conclusion, we identified 12 m6A-related lncRNAs with a potential prognostic value and developed a prognostic and predictive m6A-RLPS, which may be useful in the investigation of the functional and molecular mechanisms involved in ccRCC oncogenesis and in the determination of treatment strategies and efficacy in patients with ccRCC.

DATA AVAILABILITY STATEMENT

Publicly available datasets were analyzed in this study. These data can be found here: The Cancer Genome Atlas (<https://portal.gdc.cancer.gov/>), Gene Expression Omnibus (<https://www.ncbi.nlm.nih.gov/geo/>), and Lnc2Cancer 3.0 (<http://bio-bigdata.hrbmu.edu.cn/lnc2cancer>).

ETHICS STATEMENT

Ethical review and approval was not required for the study on human participants in accordance with the local legislation and institutional requirements. Written informed consent for participation was not required for this study in accordance with the national legislation and the institutional requirements.

AUTHOR CONTRIBUTIONS

Study concept and design: TM and YZ; data acquisition and data analysis/interpretation: TM and XW; manuscript drafting or manuscript revision for important intellectual content: TM, XL, and JW; literature study: SL, WZ, LM, and ZT. All authors contributed to the article and approved the submitted version

FUNDING

This study was supported by the National Key Research and Development Program of China (grant number: 2018YFC2002202).

ACKNOWLEDGMENTS

We would like to thank Editage (www.editage.cn) for English language editing.

SUPPLEMENTARY MATERIAL

The Supplementary Material for this article can be found online at: <https://www.frontiersin.org/articles/10.3389/fgene.2021.726369/full#supplementary-material>

REFERENCES

- Andrews, L. P., Yano, H., and Vignali, D. A. A. (2019). Inhibitory Receptors and Ligands beyond PD-1, PD-L1 and CTLA-4: Breakthroughs or Backups. *Nat. Immunol.* 20, 1425–1434. doi:10.1038/s41590-019-0512-0
- Bray, F., Ferlay, J., Soerjomataram, I., Siegel, R. L., Torre, L. A., and Jemal, A. (2018). Global Cancer Statistics 2018: GLOBOCAN Estimates of Incidence and Mortality Worldwide for 36 Cancers in 185 Countries. *CA: A Cancer J. Clinicians* 68, 394–424. doi:10.3322/caac.21492
- Cai, J., Yang, F., Zhan, H., Situ, J., Li, W., Mao, Y., et al. (2019). RNA m6A Methyltransferase METTL3 Promotes the Growth of Prostate Cancer by Regulating Hedgehog Pathway. *Ott* 12, 9143–9152. doi:10.2147/OTT.S226796
- Carosella, E. D., Ploussard, G., LeMaout, J., and Desgrandchamps, F. (2015). A Systematic Review of Immunotherapy in Urologic Cancer: Evolving Roles for Targeting of CTLA-4, PD-1/programmed cell death-1, and HLA-G. *Eur. Urol.* 68, 267–279. doi:10.1016/j.eururo.2015.02.032
- Chen, B., Khodadoust, M. S., Liu, C. L., Newman, A. M., and Alizadeh, A. A. (2018). Profiling Tumor Infiltrating Immune Cells with CIBERSORT. *Methods Mol. Biol.* 1711, 243–259. doi:10.1007/978-1-4939-7493-1_12
- Chen, J., Yu, K., Zhong, G., and Shen, W. (2020). Identification of a m6A RNA Methylation Regulators-Based Signature for Predicting the Prognosis of clear Cell Renal Carcinoma. *Cancer Cell Int* 20, 157. doi:10.1186/s12935-020-01238-3
- Chen, X.-Y., Zhang, J., and Zhu, J.-S. (2019). The Role of m6A RNA Methylation in Human Cancer. *Mol. Cancer* 18, 103. doi:10.1186/s12943-019-1033-z
- Chen, Z., Zhang, J., Zhang, Z., Feng, Z., Wei, J., Lu, J., et al. (2017). The Putative Tumor Suppressor microRNA-30a-5p Modulates clear Cell Renal Cell Carcinoma Aggressiveness through Repression of ZEB2. *Cell Death Dis* 8, e2859. doi:10.1038/cddis.2017.252
- Dalglish, G. L., Furge, K., Greenman, C., Chen, L., Bignell, G., Butler, A., et al. (2010). Systematic Sequencing of Renal Carcinoma Reveals Inactivation of Histone Modifying Genes. *Nature* 463, 360–363. doi:10.1038/nature08672
- Denaro, N., Merlano, M. C., and Lo Nigro, C. (2019). Long Noncoding RNA S as Regulators of Cancer Immunity. *Mol. Oncol.* 13, 61–73. doi:10.1002/1878-0261.12413
- Deng, X., Su, R., Weng, H., Huang, H., Li, Z., and Chen, J. (2018). RNA N6-Methyladenosine Modification in Cancers: Current Status and Perspectives. *Cell Res* 28, 507–517. doi:10.1038/s41422-018-0034-6
- Eckel-Passow, J. E., Serie, D. J., Bot, B. M., Joseph, R. W., Chevillat, J. C., and Parker, A. S. (2014). ANKS1B Is a Smoking-Related Molecular Alteration in clear Cell Renal Cell Carcinoma. *BMC Urol.* 14, 14. doi:10.1186/1471-2490-14-14
- Feng, W., Li, B., Wang, J., Zhang, H., Liu, Y., Xu, D., et al. (2020). Long Non-coding RNA LINC00115 Contributes to the Progression of Colorectal Cancer by Targeting miR-489-3p via the PI3K/AKT/mTOR Pathway. *Front. Genet.* 11, 567630. doi:10.3389/fgene.2020.567630
- Friedman, J., Hastie, T., and Tibshirani, R. (2010). Regularization Paths for Generalized Linear Models via Coordinate Descent. *J. Stat. Soft.* 33, 1–22. doi:10.18637/jss.v033.i01
- Gao, Y., Shang, S., Guo, S., Li, X., Zhou, H., Liu, H., et al. (2021). Lnc2Cancer 3.0: an Updated Resource for Experimentally Supported lncRNA/circRNA Cancer Associations and Web Tools Based on RNA-Seq and scRNA-Seq Data. *Nucleic Acids Res.* 49 (D1), D1251–D1258. doi:10.1093/nar/gkaa1006
- Ghafari-Fard, S., Dashti, S., Farsi, M., and Taheri, M. (2021). Deleted in Lymphocytic Leukemia 2 (DLEU2): an lncRNA with Dissimilar Roles in Different Cancers. *Biomed. Pharmacother.* 133, 111093. doi:10.1016/j.biopha.2020.111093
- Gu, Y., Wu, X., Zhang, J., Fang, Y., Pan, Y., Shu, Y., et al. (2021). The Evolving Landscape of N6-Methyladenosine Modification in the Tumor Microenvironment. *Mol. Ther.* 29, 1703–1715. doi:10.1016/j.yjth.2021.04.009
- Hinshaw, D. C., and Shevde, L. A. (2019). The Tumor Microenvironment Innately Modulates Cancer Progression. *Cancer Res.* 79, 4557–4566. doi:10.1158/0008-5472.CAN-18-3962
- Huang, H., Weng, H., and Chen, J. (2020). m6A Modification in Coding and Non-coding RNAs: Roles and Therapeutic Implications in Cancer. *Cancer Cell* 37, 270–288. doi:10.1016/j.ccell.2020.02.004
- Kadomoto, S., Izumi, K., Hiratsuka, K., Nakano, T., Naito, R., Makino, T., et al. (2019). Tumor-associated Macrophages Induce Migration of Renal Cell Carcinoma Cells via Activation of the CCL20-CCR6 axis. *Cancers* 12, 89. doi:10.3390/cancers12010089
- Li, W. (2012). Volcano Plots in Analyzing Differential Expressions with mRNA Microarrays. *J. Bioinform. Comput. Biol.* 10 (6), 1231003. doi:10.1142/s0219720012310038
- Li, X., Tang, J., Huang, W., Wang, F., Li, P., Qin, C., et al. (2017). The M6A Methyltransferase METTL3: Acting as a Tumor Suppressor in Renal Cell Carcinoma. *Oncotarget* 8, 96103–96116. doi:10.18632/oncotarget.21726
- Liu, J., Eckert, M. A., Harada, B. T., Liu, S.-M., Lu, Z., Yu, K., et al. (2018). m6A mRNA Methylation Regulates AKT Activity to Promote the Proliferation and Tumorigenicity of Endometrial Cancer. *Nat. Cell Biol.* 20, 1074–1083. doi:10.1038/s41556-018-0174-4
- Ljungberg, B., Albiges, L., Abu-Ghanem, Y., Bensalah, K., Dabestani, S., Fernández-Pello, S., et al. (2019). European Association of Urology Guidelines on Renal Cell Carcinoma: the 2019 Update. *Eur. Urol.* 75, 799–810. doi:10.1016/j.eururo.2019.02.011
- Manieri, N. A., Chiang, E. Y., and Grogan, J. L. (2017). TIGIT: a Key Inhibitor of the Cancer Immunity Cycle. *Trends Immunol.* 38, 20–28. doi:10.1016/j.it.2016.10.002
- Mori, K., Mostafaei, H., Miura, N., Karakiewicz, P. I., Luzzago, S., Schmidinger, M., et al. (2021). Systemic Therapy for Metastatic Renal Cell Carcinoma in the First-Line Setting: a Systematic Review and Network Meta-Analysis. *Cancer Immunol. Immunother.* 70, 265–273. doi:10.1007/s00262-020-02684-8
- Motzer, R. J., Penkov, K., Haanen, J., Rini, B., Albiges, L., Campbell, M. T., et al. (2019). Avelumab Plus Axitinib versus Sunitinib for Advanced Renal-Cell Carcinoma. *N. Engl. J. Med.* 380, 1103–1115. doi:10.1056/NEJMoa1816047
- Ni, W., Yao, S., Zhou, Y., Liu, Y., Huang, P., Zhou, A., et al. (2019). Long Noncoding RNA GAS5 Inhibits Progression of Colorectal Cancer by Interacting with and Triggering YAP Phosphorylation and Degradation and Is Negatively Regulated by the m6A Reader YTHDF3. *Mol. Cancer* 18, 143. doi:10.1186/s12943-019-1079-y
- Patil, D. P., Chen, C.-K., Pickering, B. F., Chow, A., Jackson, C., Guttman, M., et al. (2016). m6A RNA Methylation Promotes XIST-Mediated Transcriptional Repression. *Nature* 537, 369–373. doi:10.1038/nature19342
- Peng, W.-X., Koirala, P., and Mo, Y.-Y. (2017). lncRNA-mediated Regulation of Cell Signaling in Cancer. *Oncogene* 36, 5661–5667. doi:10.1038/nc.2017.184
- Powles, T., Plimack, E. R., Soulières, D., Waddell, T., Stus, V., Gafanov, R., et al. (2020). Pembrolizumab Plus Axitinib versus Sunitinib Monotherapy as First-Line Treatment of Advanced Renal Cell Carcinoma (KEYNOTE-426): Extended Follow-Up from a Randomised, Open-Label, Phase 3 Trial. *Lancet Oncol.* 21 (e553), 1563–1573. doi:10.1016/S1470-2045(20)30436-8
- Rini, B. I., Campbell, S. C., and Escudier, B. (2009). Renal Cell Carcinoma. *The Lancet* 373, 1119–1132. doi:10.1016/S0140-6736(09)60229-4
- Santagata, S., Napolitano, M., D'Alterio, C., Desicato, S., Maro, S. D., Marinelli, L., et al. (2017). Targeting CXCR4 Reverts the Suppressive Activity of T-Regulatory Cells in Renal Cancer. *Oncotarget* 8, 77110–77120. doi:10.18632/oncotarget.20363
- Shingarev, R., and Jaimes, E. A. (2017). Renal Cell Carcinoma: New Insights and Challenges for a Clinician Scientist. *Am. J. Physiology-Renal Physiol.* 313, F145–F154. doi:10.1152/ajprenal.00480.2016
- Siegel, R. L., Miller, K. D., and Jemal, A. (2020). Cancer Statistics, 2020. *CA A. Cancer J. Clin.* 70, 7–30. doi:10.3322/caac.21590
- Simonaggio, A., Epailard, N., Pobel, C., Moreira, M., Oudard, S., and Vano, Y.-A. (2021). Tumor Microenvironment Features as Predictive Biomarkers of Response to Immune Checkpoint Inhibitors (ICI) in Metastatic clear Cell Renal Cell Carcinoma (mccRCC). *Cancers* 13, 231. doi:10.3390/cancers13020231
- Strick, A., Hagen, F., Gundert, L., Klümper, N., Tolkach, Y., Schmidt, D., et al. (2020). The N 6 -methyladenosine (M 6 A) Erasers Alkylation Repair Homologue 5 (ALKBH5) and Fat Mass and Obesity-associated Protein (FTO) Are Prognostic Biomarkers in Patients with clear Cell Renal Carcinoma. *BJU Int.* 125, 617–624. doi:10.1111/bju.15019
- Tang, J., Yu, B., Li, Y., Zhang, W., Alvarez, A. A., Hu, B., et al. (2019). TGF- β -activated lncRNA LINC00115 Is a Critical Regulator of Glioma Stem-like Cell Tumorigenicity. *EMBO Rep.* 20, e48170. doi:10.15252/embr.201948170
- Taniue, K., and Akimitsu, N. (2021). The Functions and Unique Features of lncRNAs in Cancer Development and Tumorigenesis. *Ijms* 22, 632. doi:10.3390/ijms22020632

- Tian, P., Wei, J. X., Li, J., Ren, J. K., and Yang, J. J. (2021). lncRNA SNHG1 Regulates Immune Escape of Renal Cell Carcinoma by Targeting miR-129-3p to Activate STAT3 and PD-L1. *Cell Biol. Int.* 45, 1546–1560. doi:10.1002/cbin.11595
- Veeratterapillay, R., Simren, R., El-Sherif, A., Johnson, M. I., Soomro, N., and Heer, R. (2012). Accuracy of the Revised 2010 TNM Classification in Predicting the Prognosis of Patients Treated for Renal Cell Cancer in the north east of England. *J. Clin. Pathol.* 65, 367–371. doi:10.1136/jclinpath-2011-200468
- von Roemeling, C. A., Radisky, D. C., Marlow, L. A., Cooper, S. J., Grebe, S. K., Anastasiadis, P. Z., et al. (2014). Neuronal Pentraxin 2 Supports clear Cell Renal Cell Carcinoma by Activating the AMPA-Selective Glutamate Receptor-4. *Cancer Res.* 74, 4796–4810. doi:10.1158/0008-5472.CAN-14-0210
- Wang, Q., Chen, C., Ding, Q., Zhao, Y., Wang, Z., Chen, J., et al. (2020a). METTL3-mediated m6A Modification of HDGF mRNA Promotes Gastric Cancer Progression and Has Prognostic Significance. *Gut* 69, 1193–1205. doi:10.1136/gutjnl-2019-319639
- Wang, T., Kong, S., Tao, M., and Ju, S. (2020b). The Potential Role of RNA N6-Methyladenosine in Cancer Progression. *Mol. Cancer* 19, 88. doi:10.1186/s12943-020-01204-7
- Wang, X., Zhang, J., and Wang, Y. (2019). Long Noncoding RNA GAS5-AS1 Suppresses Growth and Metastasis of Cervical Cancer by Increasing GAS5 Stability. *Am. J. Transl. Res.* 11, 4909–4921.
- Wang, X., Xie, H., Ying, Y., Chen, D., and Li, J. (2020c). Roles of N6-methyladenosine (m6A) RNA Modifications in Urological Cancers. *J. Cel. Mol. Med.* 24, 10302–10310. doi:10.1111/jcmm.15750
- Wanna-Udom, S., Terashima, M., Lyu, H., Ishimura, A., Takino, T., Sakari, M., et al. (2020). The m6A Methyltransferase METTL3 Contributes to Transforming Growth Factor-Beta-Induced Epithelial-Mesenchymal Transition of Lung Cancer Cells through the Regulation of JUNB. *Biochem. Biophysical Res. Commun.* 524, 150–155. doi:10.1016/j.bbrc.2020.01.042
- Wozniak, M. B., Le Calvez-Kelm, F., Abedi-Ardekani, B., Byrnes, G., Durand, G., Carreira, C., et al. (2013). Integrative Genome-wide Gene Expression Profiling of clear Cell Renal Cell Carcinoma in Czech Republic and in the United States. *PLOS ONE* 8, e57886. doi:10.1371/journal.pone.0057886
- Xiong, Y., Wang, Z., Zhou, Q., Zeng, H., Zhang, H., Liu, Z., et al. (2020). Identification and Validation of Dichotomous Immune Subtypes Based on Intratumoral Immune Cells Infiltration in clear Cell Renal Cell Carcinoma Patients. *J. Immunother. Cancer* 8, e000447. doi:10.1136/jitc-2019-000447
- Yang, X., Hu, X., Liu, J., Wang, R., Zhang, C., Han, F., et al. (2020). N6-methyladenine Modification in Noncoding RNAs and its Function in Cancer. *Biomark. Res.* 8, 61. doi:10.1186/s40364-020-00244-x
- Yoshihara, K., Shahmoradgoli, M., Martinez, E., Vegesna, R., Kim, H., Torres-Garcia, W., et al. (2013). Inferring Tumour Purity and Stromal and Immune Cell Admixture from Expression Data. *Nat. Commun.* 4, 2612. doi:10.1038/ncomms3612
- Yuan, X., Yang, T., Xu, Y., Ou, S., Shi, P., Cao, M., et al. (2020). SNHG10 Promotes Cell Proliferation and Migration in Gastric Cancer by Targeting miR-495-3p/CTNNB1 Axis. *Dig. Dis. Sci.* 66 (8), 2627–2636. doi:10.1007/s10620-020-06576-w
- Zeng, J.-h., Lu, W., Liang, L., Chen, G., Lan, H.-h., Liang, X.-Y., et al. (2019). Prognosis of clear Cell Renal Cell Carcinoma (ccRCC) Based on a Six-lncRNA-Based Risk Score: an Investigation Based on RNA-Sequencing Data. *J. Transl. Med.* 17, 281. doi:10.1186/s12967-019-2032-y
- Zhang, J., Cao, Z., Ding, X., Wei, X., Zhang, X., Hou, J., et al. (2017). The lncRNA XIST Regulates the Tumorigenicity of Renal Cell Carcinoma Cells via the miR-302c/SDC1 axis. *Int. J. Clin. Exp. Pathol.* 10, 7481–7491.
- Zhang, J., Jin, S., Xiao, W., Zhu, X., Jia, C., and Lin, Z. (2021). Long Noncoding RNA LINC00641 Promotes Renal Cell Carcinoma Progression via Sponging microRNA-340-5p. *Cancer Cel Int* 21, 210. doi:10.1186/s12935-021-01895-y
- Zhu, S., Liu, Y., Wang, X., Wang, J., and Xi, G. (2020). lncRNA SNHG10 Promotes the Proliferation and Invasion of Osteosarcoma via Wnt/ β -Catenin Signaling. *Mol. Ther. - Nucleic Acids* 22, 957–970. doi:10.1016/j.omtn.2020.10.010
- Zuo, X., Chen, Z., Gao, W., Zhang, Y., Wang, J., Wang, J., et al. (2020). M6A-mediated Upregulation of LINC00958 Increases Lipogenesis and Acts as a Nanotherapeutic Target in Hepatocellular Carcinoma. *J. Hematol. Oncol.* 13, 5. doi:10.1186/s13045-019-0839-x

Conflict of Interest: The authors declare that the research was conducted in the absence of any commercial or financial relationships that could be construed as a potential conflict of interest.

Publisher's Note: All claims expressed in this article are solely those of the authors and do not necessarily represent those of their affiliated organizations, or those of the publisher, the editors, and the reviewers. Any product that may be evaluated in this article, or claim that may be made by its manufacturer, is not guaranteed or endorsed by the publisher.

Copyright © 2021 Ma, Wang, Wang, Liu, Lai, Zhang, Meng, Tian and Zhang. This is an open-access article distributed under the terms of the Creative Commons Attribution License (CC BY). The use, distribution or reproduction in other forums is permitted, provided the original author(s) and the copyright owner(s) are credited and that the original publication in this journal is cited, in accordance with accepted academic practice. No use, distribution or reproduction is permitted which does not comply with these terms.